Synthetic and Systems Biotechnology 9 (2024) 766–774

Contents lists available at ScienceDirect

Synthetic and Systems Biotechnology

journal homepage: www.keaipublishing.com/en/journals/synthetic-and-systems-biotechnology

Original Research Article

Stepwise increase of fidaxomicin in an engineered heterologous host *Streptomyces albus* through multi-level metabolic engineering

Huang Xie [a,b], Yi-Ting Su [a,b], Qing-Ting Bu [a,b], Yue-Ping Li [a,b], Qing-Wei Zhao [a], Yi-Ling Du [a,b,**], Yong-Quan Li [a,b,*]

[a] First Affiliated Hospital and Institute of Pharmaceutical Biotechnology, Zhejiang University School of Medicine, Hangzhou 310058, China
[b] Zhejiang Provincial Key Laboratory for Microbial Biochemistry and Metabolic Engineering, Hangzhou 310058, China

ARTICLE INFO

Keywords:
Fidaxomicin
Heterologous expression
Streptomyces albus
Genome-reduced chassis
Metabolic engineering

ABSTRACT

The anti-*Clostridium difficile* infection (CDI) drug fidaxomicin is a natural polyketide metabolite mainly produced by *Micromonosporaceae*, such as *Actinoplanes deccanensis*, *Dactylosporangium aurantiacum*, and *Micromonospora echinospora*. In the present study, we employed a stepwise strategy by combining heterologous expression, chassis construction, promoter engineering, activator and transporters overexpression, and optimization of fermentation media for high-level production of fidaxomicin. The maximum yield of 384 mg/L fidaxomicin was achieved with engineered *Streptomyces albus* D7-VHb in 5 L-tank bioreactor, and it was approximately 15-fold higher than the native strain *Actinoplanes deccanensis* YP-1 with higher strain stability and growth rate. This study developed an enhanced chassis strain, and for the first time, achieved the heterologous synthesis of fidaxomicin through a combinatorial metabolic engineering strategy.

1. Introduction

Fidaxomicin (FDX), a natural polyketide metabolite principally synthesized by *Actinoplanes deccanensis*, *Dactylosporangium aurantiacum*, *Micromonospora echinospora*, and *Catellatospora* species [1], emerges as a beacon of hope in the battle against *Clostridium difficile* infection (CDI). In 2011, FDA endorsed FDX under the trade name Dificid, for the clinical management of CDI. Demonstrating a superior efficacy profile, FDX not only substantially reduces the recurrence of infection but also ensures a higher likelihood of complete recovery when compared to traditional treatments like vancomycin and metronidazole [2,3], thereby asserting its potential as the primary treatment modality for CDI. Intriguingly, FDX has also shown promising antitumor properties, with certain derivatives exhibiting enhanced antibacterial activity against pathogens such as *Staphylococcus aureus*, *Micrococcus luteus*, and *Enterococcus faecalis* [4]. This positions FDX as a cornerstone in the realm of pharmaceutical development. However, the intricate structure of FDX presents a formidable challenge to chemical synthesis [5], making microbial fermentation the predominant method for its production. The elucidation of the biosynthetic pathway in *A. deccanensis* and *D. aurantiacum*, encompassing over 30 genes across approximately 100 kb of their genomes, marks a significant milestone in understanding the biosynthetic machinery of this potent molecule [6,7].

The native producer of FDX, *Actinoplanes deccanensis* YP-1, is characterized by its inability to form spores, slow growing, and strain degeneration subsequent to serial cultivation, which imposed significant limitations on its utility [8]. Moreover, the yield of FDX remains insufficient to meet commercial requirement. As a remedial strategy, the heterologous expression of the FDX gene cluster within highly efficient and stable hosts may circumvent the inherent deficiencies of its native producers. Coinciding with the strides in synthetic biology, a plethora of robust and refined host platforms have been crafted through extensive genome reduction strategies, encompassing species such as *Escherichia coli*, *Bacillus subtilis*, *Pseudomonas putida*, *Aspergillus nidulans*, *Saccharomyces cerevisiae*, *Streptomyces albus*, *Streptomyces coelicolor* and *Streptomyces avermitilis* [9]. Typically, the heterologous expression of a biosynthetic gene cluster (BGC) within taxonomically disparate host strains presents considerable challenges, attributed to variations in codon usage, GC content, and the availability of precursors. Given that *A. deccanensis* is a member of the actinomycetes genus, the *Streptomyces*

Peer review under responsibility of KeAi Communications Co., Ltd.
* Corresponding author;First Affiliated Hospital and Institute of Pharmaceutical Biotechnology, Zhejiang University School of Medicine, Hangzhou 310058, China
** Corresponding author;First Affiliated Hospital and Institute of Pharmaceutical Biotechnology, Zhejiang University School of Medicine, Hangzhou 310058, China.
E-mail addresses: yldu@zju.edu.cn (Y.-L. Du), lyq@zju.edu.cn (Y.-Q. Li).

https://doi.org/10.1016/j.synbio.2024.06.004
Received 30 April 2024; Received in revised form 28 May 2024; Accepted 12 June 2024
Available online 17 June 2024

species emerges as the theoretically preferred hosts among the aforementioned candidates for the heterologous expression of FDX.

In this study, by employing BAC construction and PCR screening methodologies, we successfully isolated the entire BGC responsible for the synthesis of FDX *in vitro*. This gene cluster was subsequently conjugatively transferred to and productivity assessed within a selection of high-caliber *Streptomyces* chassis strains that are prevalently employed within the sphere of microbial engineering, thereby discerning *Streptomyces albus* J1074 as the quintessential host for the heterologous production of FDX. Targeting this specific host, we employed the CRISPR/Cpf1 technology to effectuate the large-scale deletion of 6 BGCs and 2 GIs (genomic islands), cumulatively excising 358 kb of superfluous sequences. Concurrently, we integrated the *vgb2* gene encoding *Vitreoscilla* hemoglobin, resulting in the creation of an enhanced chassis strain, D7-VHb, with superior traits. Through strategies such as promoter engineering and *in situ* replacement, adaptive selection of regulatory factors, overexpression of efflux genes, and combinatorial precursor engineering, for the first time we achieved stable and rapid production of FDX in an engineered heterologous host.

2. Material and methods

2.1. Strains, plasmids, primers, and culture conditions

Bacterial strains and plasmids used in this study were listed in Table S1, and primers were listed in Table S2 in the supplementary materials. *E. coli* TG1 was used as host for plasmid construction. *E. coli* DH10B or GB05 was used for the propagation of large plasmid DNA. *E. coli* ET12567/pUZ8002 and *E. coli* ET12567/pUB307 were used as donor for intergeneric conjugation to *S. albus* J1074 or its mutants. The components of media for *S. albus* were as follows, YEME (0.3 % yeast extract, 0.3 % malt extract, 0.5 % tryptone, 4 % glucose); R5A (9.5 % sucrose, 1.0 % glucose, 0.4 % glucose, 0.5 % yeast extract, 2 % MOPS, 0.01 % casamino acids, 1 % $MgCl_2$, 0.02 % K_2SO_4, 2 mL trace element solution, pH 6.8–7.2); INM1 (2 % glucose, 1.84 % soluble starch, 0.5 % yeast powder, 1.75 % soluble cottonseed cake powder, 0.728 % K_2HPO_4, 0.25 % NaCl, pH 6.8–7.2); INM2 (5 % maltodextrin, 2.5 % corn starch, 1.5 % glucose, 1.5 % soybean cake powder, 1 % dry corn syrup powder, 1 % yeast powder, 0.05 % K_2HPO_4, 0.05 % KH_2PO_4, 0.3 % $CaCO_3$, 0.3 % soybean oil, pH 6.8–7.2); INM3 (5 % sucrose, 2.5 % sorbitol, 2.5 % glycerol, 0.3 % soy oil, 1 % soybean cake powder, 0.5 % yeast powder, 0.5 % gluten meal, 0.3 % $CaCO_3$, 0.2 % $MgCl_2$, 0.2 % KCl, 0.05 % KH_2PO_4, pH 6.8–7.2); TSB (3 % TSB, BD Biosciences). If needed, antibiotics were supplemented to growth media at the following concentrations: 100 μg/mL ampicillin, 50 μg/mL apramycin, 25 μg/mL chloramphenicol, 25 μg/mL thiostrepton, 50 μg/mL kanamycin, 30 μg/mL nalidixic acid.

2.2. Plasmid construction and transformation

CRISPR/Cpf1-mediated genome editing method was used to construct the deletion mutants of *S. albus* J1074. The primers and restriction sites used were listed in Table S2. Homology arm A and B are set to 500–1000 bp, and the 23-nt protospacer sequences targeting the deletion regions were designed by sgRNA Scorer 2.0 or CHOPCHOP website with PAM TTV at its 5′ end as described previously [10]. The successfully built plasmids were introduced into ET12567/pUZ8002. After conjugal transfer with *S. albus*, exconjugants were selected on MS (10 mM $MgCl_2$ added) plate with apramycin and nalidixic acid. To remove the plasmid with resistance tag, knock-out strains were grown on MS medium without apramycin at 37 °C for two rounds.

For construction of the combined overexpression vector, the *pank*, *fadT1T2* and *scnRII* genes were amplified with overlaps (15–20 bp), and then ligated into pSOK866 (digested with *Eco*RI) using a ClonExpress MultiS One Step Cloning Kit (Vazyme, China) to obtain pSOK866-Com. The resultant plasmid was confirmed by PCR and DNA sequencing. The constructed plasmids were introduced into *E. coli* ET12567/pUZ8002 for *E. coli-Streptomyces* conjugation. The *E. coli-Streptomyces* conjugation was carried out according to the standard procedures [11].

2.3. Heterologous expression of FDX BGC

In consideration of the great difficulty in directly grasping large BGCs over 100 kb, the high-quality BAC library of *Actinoplanes deccanensis* YP-1 was constructed using the BAC vector pMSBBAC1 [12] by Eight Star Bio-tech company (Wuhan China). The pMSBBAC vector contains the *oriT*, *φC31*, *attP* and *aac(3)IV* elements from pSET152 vector, which can be directly used for conjugation transfer. The positive clone p6-I-18 containing the FDX BGC was screened out by mixed PCR with primers *fad*-leftborder-F/R and *fad*-rightborder-F/R (Table S2). Through site-specific recombination, *S. albus* J1074, *S. coelicolor* M1154, *S. avermitilis* SUKA22 and *S. albus* D7-VHb were successfully used as the hosts for heterologous expression. *E. coli* ET12567/pUB307 [13] was used as the helper strains for the triparental mating.

2.4. Modification of BGC using Red/ET recombination technology

Firstly, *E. coli* GB05RedTrfA [14] harboring the pSC101-BAD-ETgA-tet plasmid was inoculated into 6 mL LB medium supplemented with tetracycline (5 μg/mL). The culture was incubated at 30 °C, 220 rpm overnight. Sterile Eppendorf tubes with perforated caps were used to aliquot 1.4 mL of LB medium (tetracycline added) and inoculated with 20–40 μL of the bacterial culture. Incubation continued at 30 °C, 220 rpm for about 2 h until OD_{600nm} reached 0.4. L-Arabinose was added at a final concentration of 1 % as an inducer and the culture was transferred to 37 °C until the OD_{600nm} reached 0.8, for about 40 min. Cells were then pelleted by centrifugation at 7500 rpm, and the pellet was resuspended in 1 mL of 10 % sterile glycerol. After another centrifugation at 7500 rpm for 1 min and discarding the supernatant, the cells were washed once more. The washed pellet was resuspended in 40 μL of 10 % glycerol, followed by the addition of 10 μL of the transformation mix containing 2 μL plasmid (pMSBBAC1-*fad*) and 8 μL fragment (promoters with ampicillin label). Electroporation was performed immediately thereafter. Subsequently, 750 μL of LB was added, and the mixture was incubated at 37 °C for 1 h before being spread on LB plates. The transformants were confirmed by PCR and DNA sequencing.

2.5. Detection of FDX by high-pressure liquid chromatography (HPLC)

The fermentation samples (200 μL) were harvested at certain time points and extracted with 800 μL methanol overnight. The mixed solutions were centrifuged at 15,000 rpm for 10 min, and then the supernatants were injected into HPLC (Shimadzu, LC-20ADXR) equipped with a 4.6 × 150 mm Agilent Poroshell 120 EC-C18 (600 bar/2.7 μm) column to measure the FDX titer. For HPLC detection, acetonitrile/water (0.08 % trifluoroacetic acid added) gradient was used as the mobile phase: 0 min, 34 % acetonitrile; 20 min, 90 % acetonitrile; 25 min, 90 % acetonitrile; 28 min, 34 % acetonitrile; 35 min, 34 % acetonitrile. The flow rate was 1.0 mL/min and FDX eluted at approximately 17.5 min. The eluate was monitored at 254 nm, and the column temperature was set at 37 °C.

2.6. Measurement of intracellular ATP, and NADPH/$NADP^+$ ratio

To ascertain the intracellular concentrations of ATP, and NADPH/$NADP^+$ in *S. albus* J1074 and its derivative mutants, cultures were grown in YEME medium. Post-incubation, mycelial samples were harvested via centrifugation and subjected to dual washes with PBS buffer. Subsequent quantification of intracellular ATP, and NADPH/$NADP^+$ levels was conducted utilizing ATP and NADP(H) assay kits (Solarbio), strictly adhering to the supplier's guidelines. Additionally, biomass or dry cell mass (DCM) determinations were carried out. The concentrations were

calculated by measured content (μmol)/DCM (g). To ensure reproducibility, all experimental procedures were executed in triplicate.

2.7. Quantitative measurement of total XylE activity

Mycelia from strains harboring the XylE-reporter were harvested following one or two-day cultivation in YEME media via centrifugation at 12,000 rpm for 2 min. The resulting cell pellets underwent two rounds of washing with distilled water before being resuspended in a lysis buffer composed of 100 mM phosphate buffer saline (PBS) at pH 7.5, 20 mM EDTA at pH 8.0, and 10 % (v/v) acetone. Cell lysates were then produced by sonication on ice (3 cycles of 2 s each, with 3-s intervals between cycles). Triton X-100 was subsequently introduced to achieve a final concentration of 0.1 % (v/v). After centrifuging the lysates at 12,000 rpm for 2 min at 4 °C, the supernatants were collected into a new tube. A volume of 100 μL of these supernatants was added to 900 μL of a pre-warmed assay buffer (10 mM PBS and 0.2 mM catechol). This reaction mixture was then incubated at 30 °C for 10 min, after which the absorbance at 375 nm was determined using spectrophotometer. The activity of catechol dioxygenase was quantified by calculating the rate of change in optical density at 375 nm, with results expressed in milliunits/mg of total protein.

3. Results

3.1. Heterologous expression of FDX-BGC in various streptomyces hosts

The yield of FDX in the native producer YP-1 is 25 mg/L, and more crucially the production of FDX by native strains is susceptible to reduction or even complete loss during the preservation and propagation processes, beset by considerable genetic instability. To address this issue, we pivoted our strategy towards the heterologous expression of FDX-BGC in commonly used *Streptomyces* hosts. Initially, we constructed and screened a genomic library, yielding the plasmid pMSBBAC1-*fad* (~120 kb) containing the FDX-BGC, whose integrity was confirmed via PCR (Fig. S1). As shown in Fig. 1A, the core scaffold of FDX is synthesized by 4 polyketide synthases (A1-A4), and side groups are added by multiple post-modification enzymes (S5, S6, P1, P2, etc.). Subsequently, we endeavored to introduce the plasmid containing FDX-BGC into five prevalent *Streptomyces* hosts, namely *S. albus* ZXJ-6 [15], *S. chattanoogensis* L321 [16], *S. albus* J1074 [17], *S. coelicolor* M1154 [18], and *S. avermitilis* SUKA22 [19]. Despite multiple rounds of optimization, including adjustments of Mg^{2+} and Ca^{2+} concentrations, ATP supplementation, and increased donor cell quantities, the plasmid pMSBBAC1-*fad* failed to be introduced into *S. albus* ZXJ-6 and

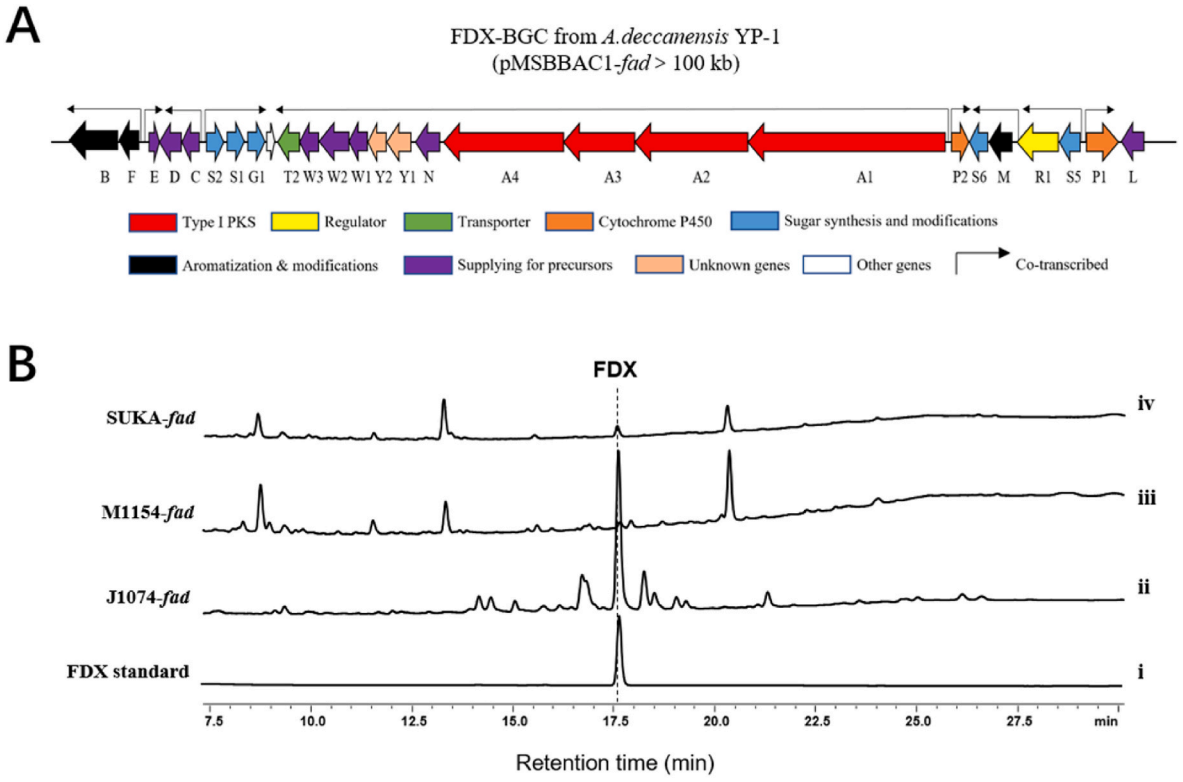

C

Various hosts	Strains	FDX yield	Chemical structure of FDX
A. deccanensis YP-1	YP-1	25 mg/L	
S. albus J1074	J1074-*fad*	35 mg/L	
S. avermitilis SUKA22	SUKA22-*fad*	<1 mg/L	
S. coelicolor M1154	M1154-*fad*	<1 mg/L	
S. albus ZXJ-6	*	/	
S. chattanoogensis L321	*	/	

Fig. 1. FDX production in several streptomyces heterologous hosts. (A) The schematic diagram of the FDX BGC. (B) The peak of FDX in different hosts viewed by HPLC assay. (C) Quantification of FDX in heterologous and native hosts. Asterisk indicates that no conjugates were obtained.

S. chattanoogensis L321. Only *S. albus* J1074, *S. coelicolor* M1154, and *S. avermitilis* SUKA22 yielded a scant number of transformants on their conjugation transfer media, identified as J1074-*fad*, M1154-*fad*, and SUKA22-*fad*, respectively. To verify FDX production, culture filtrate was then subjected to HPLC analysis. As depicted in Fig. 1B and C, the production levels of FDX in strains M1154-*fad* and SUKA22-*fad* did not reach mg/L levels. In contrast, only J1074-*fad* exhibited significant production, approximately 35 mg/L, slightly surpassing the yield of the native producing strain YP-1 in YEME medium (25 mg/L). These results underscore *S. albus* J1074 as a prime candidate chassis for the conjugation transfer of large plasmids exceeding 100 kb and for the production of FDX.

3.2. Construction of a *S. albus* chassis with superior traits

Based on the results of antiSMASH [20] (BGCs predicting server, Table S3) and IslandViewer4 (GIs predicting server, Table S4), we identified 2 Type I Polyketide Synthases (PKS), 2 Non-Ribosomal Peptide Synthetases (NRPS), 2 terpenes, and 2 genomic island regions to be deleted as shown in Table S5. Here, the selected BGCs may compete with

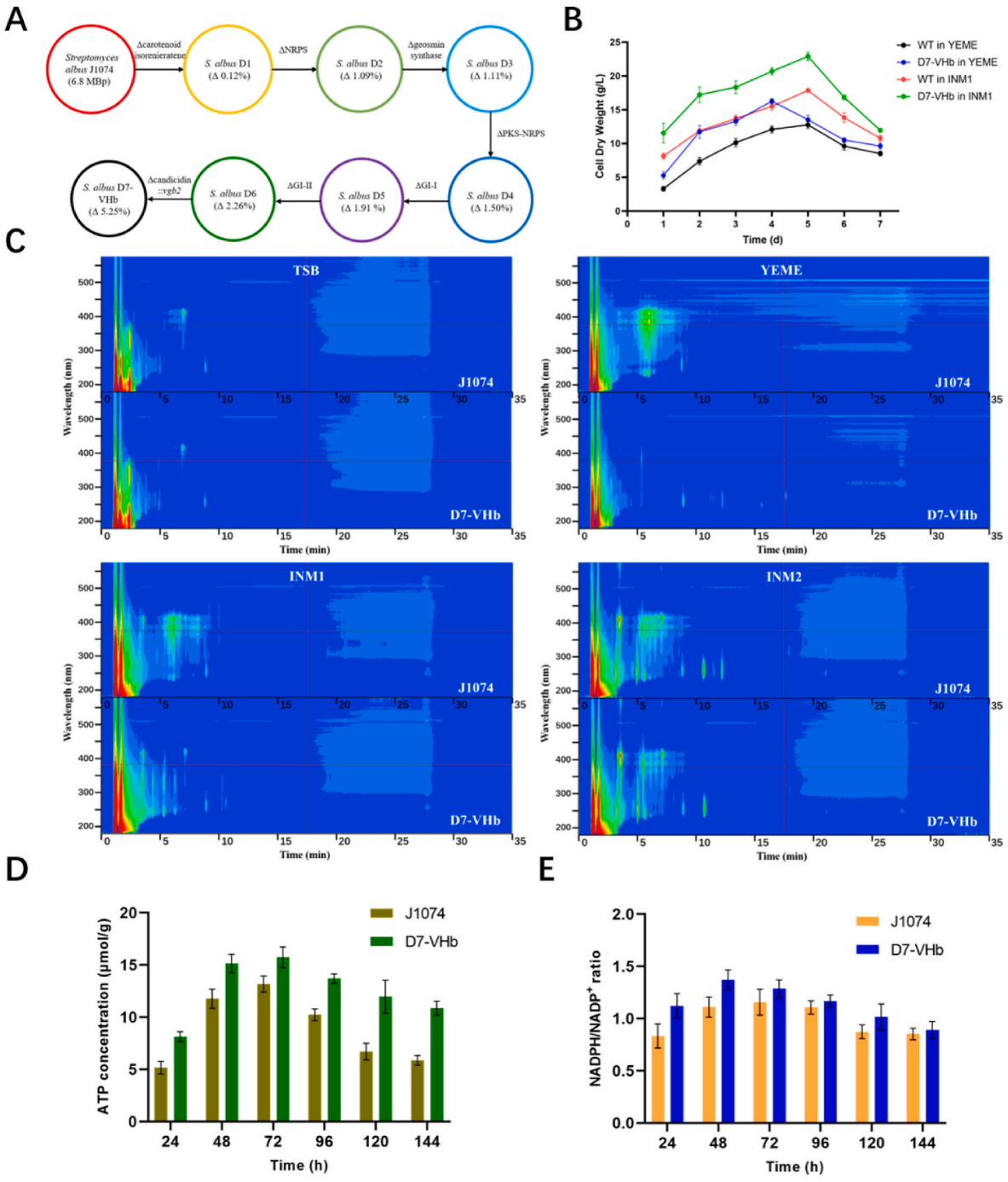

Fig. 2. The construction and performance evaluation of chassis strain D7-VHb. (A) The construction process of a streamlined and efficient chassis D7-VHb. (B) Dry weight curves of *S. albus* J1074 and D7-VHb strains. (C) Metabolite profiles analysis based on iso-absorbance plot. In the four different culture media of TSB, YEME, INM1 and INM2, J1074 and Del7-VHb were cultured for 5 days. (D) Intracellular ATP content of strain J1074 and D7-VHb. (E) Intracellular NADPH/$NADP^+$ ratio of strain J1074 and D7-VHb.

PKSs for precursors or are reported in literature as dominant BGCs, the knockout of which can significantly simplify the metabolic profile. Additionally, the chosen GIs are two largest genomic islands, potentially containing numerous unstable elements. Employing the precision of CRISPR/Cas12a-mediated gene editing, we deleted approximately 358 kb "superfluous" sequence, constituting 5.25 % of the whole genome. Concurrently, we introduced a VHb (*Vitreoscilla* hemoglobin) protein gene (*vgb2*, under the control of *ermEp**) in place of the excised candicidin gene cluster, resulting in the creation of the D7-VHb chassis strain, as depicted in Fig. 2A. Here, VHb functions as an oxygen carrier, facilitating the proliferation of microorganisms in environments characterized by diminished levels of dissolved oxygen. The expression of VHb in a heterologous system has been demonstrated to augment the efficiency of oxygen utilization, thereby elevating the production of metabolites [21–23]. These series of genetic modifications were subsequently confirmed through PCR, verifying both the deletion and insertion of genes (Fig. S2).

Generally knocking out unnecessary BGCs and GIs can significantly enhance the performance of microbial strains [24,25]. However, in certain instances, genomic reduction may hinder growth or metabolic pathways [16]. Thus, we conducted a performance evaluation of the engineered D7-VHb strain. It was observed that the growth curves of D7-VHb in both YEME and INM1 media surpassed those of J1074, especially in the nutrient-rich industrial medium INM1 (Fig. 2B). Meanwhile, we observed that D7-VHb exhibited a markedly enhanced sporulation capacity in the early phase. We examined the HPLC metabolite profiles of D7-VHb and J1074 across various media, including TSB, YEME, INM1, and INM2. Through wavelength scanning and iso-absorbance plot analysis, we found that D7-VHb possessed cleaner and simpler metabolite profiles than its parental strain J1074, especially in YEME and INM1 (Fig. 2C). As we know, ATP serves as a biological energy source for numerous intracellular reactions, and NADPH is essential as a reducing agent in various biosynthetic pathways [26]. Subsequent investigations into the intracellular ATP and NADPH/$NADP^+$ ratios of D7-VHb and J1074 revealed that D7-VHb maintained higher levels of these crucial metabolic indicators (Fig. 2D and E). Consequently, the enhanced cellular energy and reducing power in D7-VHb may contribute to an increased production of FDX. Collectively, D7-VHb strain acts to be an excellent chassis for the expression of heterologous proteins or gene clusters.

3.3. Promoter and BGC engineering to improve FDX production

We translocated the FDX BGC into the chassis strain D7-VHb through conjugation, resulting in a mutant strain named D7-VHb-*fad*. Fermentation results indicate that the D7-VHb-*fad* mutant exhibited an average fermentation yield of 46 mg/L in YEME medium over 5 days, representing a 31 % enhancement over the J1074-VHb-fad strain and an 84 % increase compared to the fermentation levels of YP-1. Moreover, in comparison to the native strain YP-1, both J1074-*fad* and D7-VHb-*fad* maintained significantly higher levels of FDX titers across consecutive passages, as illustrated in Fig. 3A.

Owing to the significant influence of gene promoter sequences on the recognition efficiency of RNA polymerase (RNAP), they consequently determine the levels of gene expression. Thus, we have selected a series of constitutive strong promoters like *ermEp**, *kasOp**, *hrdBp*, *sap6*, *sap15*, *sap 28*, *orf5354p*, *orf7707p*, *orf8238p*, *rpsL(XC)*, *gap(EL)* and *p23119*, as detailed in Table S6, intended for the promoter substitution in the FDX BGC. Herein, we employ the gene *xylE* encoding catechol-2,3-dioxygenase, to characterize the relative strengths of promoters within the chassis D7-VHb. As depicted in Fig. 3B, based on the relative activity data of XylE, it is evident that the promoters *rpsL(XC)*, *sap15*, *orf5354p*, and *sap6* exhibit relatively high activities in the strain D7-VHb.

Consequently, we designed primers to amplify a fusion of *rpsL(XC)*, *sap15*, *orf5354p*, *sap6*, *ermEp** (as control) with the ampicillin resistance gene, obtaining five fragments for electroporation. Utilizing RED/ET technology, we aimed to accomplish the *in situ* substitution of the promoter preceding the pathway-specific positive regulator gene *fadR1*. Ultimately, we successfully got 4 recombinant plasmids (excluding *sap15*) with potent promoters substituted, which were then introduced into the chassis D7-VHb for fermentation to assay FDX production. As shown in Fig. 3C, the substitution of the promoters *rpsL(XC), orf5354p*, *ermEp** significantly enhanced the fermentation yield of FDX. Inconsistent with the results in Fig. 3B, *ermEp* in situ* substitution, compared with *sap6* and *orf5354p*, showed excellent compatibility and much stronger influence on FDX yield, which may result from complicated genomic position and regulatory effects [27]. Notably, the promoter *rpsL (XC)* demonstrated a pronounced effect, with an average yield reaching 74.5 mg/L, marking a 55.2 % increase compared to the concurrent control (D7-VHb-*fad*). The mutant strain derived from the substitution of this potent *rpsL(XC)* promoter was named as D7-VHb-E*fad*.

3.4. Overexpression of adaptable regulator and transport of FDX

Each actinomycetes host evolves a unique cascade regulatory network through genetic processes to adapt to various environmental changes and respond to stress. In the original host *A. deccanensis* YP-1, the production of FDX can be increased nearly 4-fold by high expression of the pathway-specific regulatory gene *fadR1* [7]. However, the increase achieved by employing a strong promoter *in situ* replacement strategy in D7-VHb is comparatively lower. We hypothesize that the functionality of the FadR1 protein may be subject to pleiotropic regulation or modification, failing to fully manifest in heterologous hosts. Additionally, FadR1 belongs to the LuxR family within the LAL family, where the majority of studied proteins are pathway-specific positive regulators, such as FkbN in *Streptomyces tsukubaensis* [28] and RapH in *Streptomyces hygroscopicus* [29], forming a natural repository of regulatory factors. Studies have shown that LuxR family regulators exhibit a

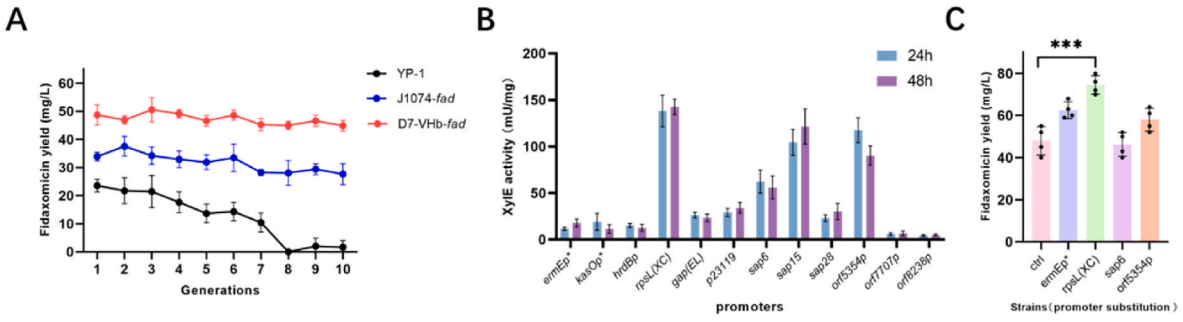

Fig. 3. FDX titers in different hosts and *in situ* replacement of screened promoters. (A) Fermentation analysis of YP-1, J1074-*fad* and D7-VHb-*fad* in YEME medium from the first generation to the tenth generation. (B) Determination of effective promoters using XylE reporter system in D7-VHb. The height of the column indicates the strength of the promoter. Error bars indicate the standard deviation of three replicates. (C) FDX titers under *in situ* replacement of several strong promoters upstream of pathway-specific regulator gene *fadR1*.

consistent regulatory pattern across different polyketide-producing strains. The regulated genes are responsible for the synthesis of polyketide chains, hydrolysis of sugars, and genes for ABC transport proteins, among others, serving as targets of regulation [30].

As illustrated in Table S7, we selected 6 LuxR family pathway-specific positive regulators: FadR1, FkbN, RapH, SlnR, ScnRII, and TiaR. We cloned their genes into the pSOK866 high-expression integrative vector (*ermEp** promoter, VWB integrase site, thiostrepton and apramycin resistance) and subsequently introduced the recombinant plasmids into D7-VHb-E*fad* via conjugative transfer, resulting in 6 mutant strains. Their production was verified through YEME fermentation. As depicted in Fig. 4A, the introduction of the transcription factors FkbN, RapH, and SlnR into the strains did not result in a significant change in production. However, the introduction of FadR1, ScnRII, and TiaR1 into the D7-VHb-E*fad* strains led to an upregulation in FDX production, with the overexpression of the *scnRII* gene being the most significant, resulting in a 28 % increase in yield. In contrast, overexpression of FadR1 only resulted in a 15 % increase in yield. This suggests that the ScnRII protein has a better adaptability in activating FDX production in the D7-VHb-E*fad* strain. According to Fig. 4B, upon analyzing the HTH structural domains of these proteins, we discovered that the ScnRII protein has the lowest identity, yet shares a similar 5′-AGGG-3′ DNA-binding motif with FadR1, which may also participate in the specific regulation of the FDX gene cluster [31]. Furthermore, the molecular weight of the ScnRII protein is only 31.6 kDa, compared to 94.8 kDa for the FadR1 protein, suggesting a more efficient transcription and translation mechanism might be involved in the secondary metabolic regulatory network of *Streptomyces albus*.

The cytotoxicity of secondary metabolites is a significant limitation in heterologous production, as high-yielding heterologous hosts often suffer poor growth or even apoptosis due to the lack of corresponding efflux proteins or detoxification mechanisms. Similarly, during the fermentation process of the strain D7-VHb-E*fad*, we measured the intracellular and extracellular FDX content and found that nearly 80 % accumulated inside the cells. During the fermentation process, we observed that the accumulation of FDX and its active precursors had a considerable toxic side effect on *Streptomyces albus* (data not shown). Based on these findings, we attempted to enhance the efflux of FDX and reduce its extracellular toxicity by simultaneously overexpressing the efflux gene *fadT1T2*, and adding 1 % macroporous adsorbent resin XAD-16 to the culture medium. We cloned the efflux protein genes *fadT1* and *fadT2* from YP-1 into the vector pSOK866 and introduced them into D7-VHb-E*fad*, resulting the strain D7-VHb-E*fad*-T1T2. The strain was fermented alongside J1074-*fad*, D7-VHb-*fad*, and D7-VHb-E*fad*, with intracellular and extracellular contents measured. As shown in Fig. 4C, the fermentation level of the strains with *fadT1T2* introduced increased by 24 % compared to D7-VHb-E*fad*, with an 11 % reduction in intracellular FDX content. Furthermore, the fermentation level of D7-VHb-E*fad*-T1T2 with XAD-16 added (E*fad*-T1T2*) reached 121 mg/L, totaling a 73 % increase in yield and a 37 % reduction in intracellular content.

3.5. Combinatorial metabolic engineering to construct heterologous high-yield system

Pantothenate is a key precursor in the biosynthesis of Coenzyme A, with Pantothenate kinase (Pank) catalyzing the phosphorylation of pantothenate to 4′-phosphopantothenate, the initial step in Coenzyme A biosynthesis. Overexpression of the *panK* gene in *S. coelicolor* and *S. peucetius* respectively resulted in a 1.5-fold increase in actinorhodin production and a 1.4-fold increase in doxorubicin production [32]. Building on previously successful high-yield strategies, we conducted fusion PCR of the genes *pank*, *fadT1T2*, and *scnRII*, and inserted them into the pSOK866 vector for tandem high expression. This was followed by conjugative transfer to D7-VHb-E*fad*, with the mutant strain named D7-VHb-E*fad*-Com. This strain reached a production yield of 140 mg/L under YEME (+XAD16) fermentation conditions.

Subsequently, we cultured strain D7-VHb-E*fad*-Com in five commonly used *Streptomyces* fermentation media: YEME, R5A, INM1, INM2, and INM3 (all with 1 % XAD16 added), with J1074-*fad* serving as the control. As illustrated in Fig. 5A, D7-VHb-E*fad*-Com achieved its highest yield in industrial medium INM1, reaching 189 mg/L, which is a 223 % increase over J1074-*fad* under identical cultivation conditions. Following this, we carried out a scale-up experiment in a 5 L fermenter using industrial medium INM1. As shown in Fig. 5B, J1074-*fad* reached its peak yield of 98 mg/L after 6 days of fermentation. In comparison, the strain D7-VHb-E*fad*-Com exhibited rapid growth after inoculation,

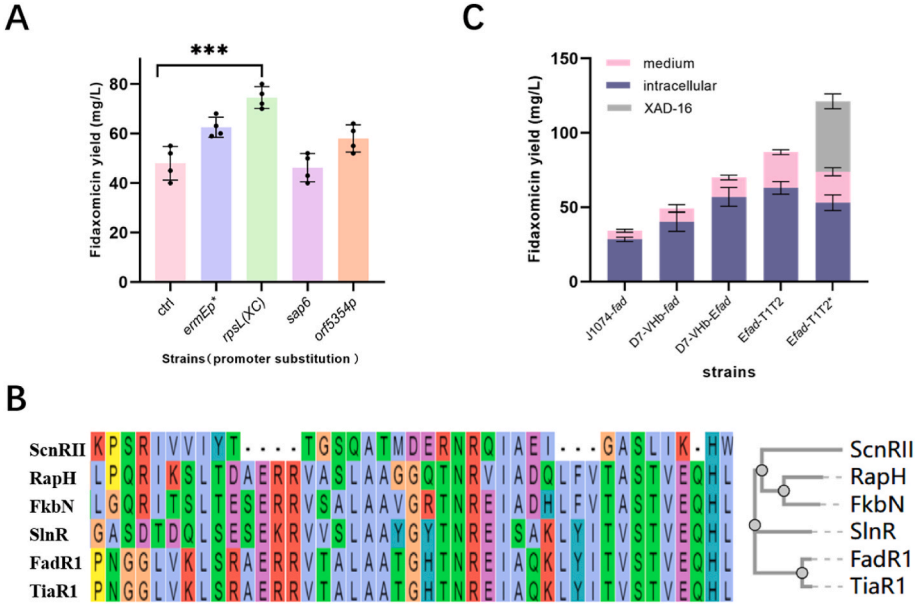

Fig. 4. Adaptable transcriptional regulator screening and transport of intracellular FDX. (A) FDX titers of various LuxR family transcriptional regulators overexpressed in D7-VHb-E*fad*. Error bars indicate the standard deviation of four replicates. (B) Alignment and phylogenetic tree based on Helix-Turn-Helix domains of LuxR family transcriptional regulators. (C) The influence of overexpressing transporter genes *fadT1T2* (E*fad*-T1T2) and adding macroporous resin XAD-16 (marked with an asterisk).

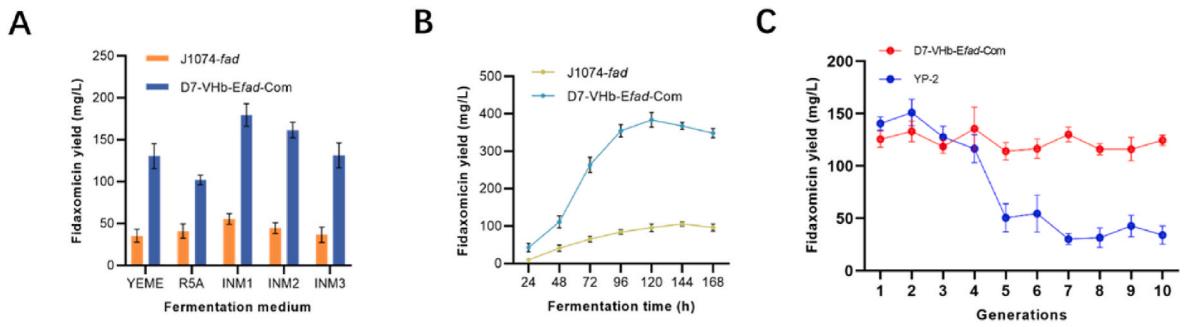

Fig. 5. Combinatorial metabolic engineering strategy to achieve heterologous hyperproduction of FDX. (A) Schematic illustration of the combinatorial strategy. BGC, biosynthetic gene cluster; VHb, *Vitreoscilla* hemoglobin; *vgb2*, a gene encoding protein VHb; pKCCpf1, a knockout vector; pMSBBAC1, BAC library vector; pSOK866, an overexpression vector; *acc(3)IV*, apramycin resistance gene; *tsr*, thiostrepton resistance gene. (B) FDX titers of J1074-*fad* and D7-VHb-E*fad*-Com under varying YEME, R5A, INM1, INM2 and INM3 fermentation media; (C) FDX titers of strain J1074-*fad* and D7-VHb-E*fad*-Com in 5-L bioreactor. (D) Analysis of FDX metabolic stability of high-yield strain YP-2 and D7-VHb-E*fad*-Com.

reaching a peak yield of 384 mg/L after 5 days of fermentation, marking an approximate 300 % increase.

In the 5 L fermenter experiment, ensuring adequate dissolved oxygen conditions significantly enhanced both the growth and FDX production of the strain D7-VHb-E*fad*-Com. The production peaked a day earlier than the wild-type control strain at 384 mg/L. Through the entire combinatorial metabolic engineering overhaul, the production of FDX increased nearly 10-fold compared to the initial yield. Additionally, we conducted serial passaging of the strain D7-VHb-E*fad*-Com and the original high-yield strain YP-2 [7], assessing the intergenerational variation in peak production during fermentation in YEME medium. As depicted in Fig. 5C, the fermentation level of FDX in strain YP-2 showed a certain degree of decline in the 3rd and 4th generations (reaching 17 %), with a sharp decrease in secondary metabolite levels from the 5th generation onwards, ranging between 61% and 78 %, while concurrent microscopic examination revealed no contamination. In contrast, strain D7-VHb-E*fad*-Com was able to maintain a stable level of FDX metabolism throughout the passaging process. Thereby we established a system for the stable and rapid heterologous production of FDX.

4. Discussion

In the realm of pharmaceutical manufacturing, the application of fermentation stands out as a notably advantageous and effective strategy for the production of structurally complex microbial medications, which are otherwise difficult or expensive to synthesize via chemical methodologies [33]. However, during industrial production processes, some microbial strains can experience low titers, reduction or even loss in the synthesis capability of the target product after prolonged preservation and continuous passage, posing obstacles to the scaled production and application of microbial drugs. Beyond enhancing the genetic stability of original drug-producing microbes such as knocking out elements that cause genetic instability (endogenous CRISPR/Cas systems, nucleases, etc.), GIs containing a large number of “jumping genes" and optimizing culture conditions, seeking out heterologous hosts with superior performance presents a viable alternative. In *S. coelicolor* M1152, researchers achieved overproduction of polyketide oviedomycin, through heterologous expression, promoter restructuring, and genome-scale metabolic simulation-assisted strategies [34]. Similarly, efficient expression of herbicide thaxtomin was achieved through strategies such as heterologous expression, repression protein deficiency, transcription factor overexpression, and fermentation medium optimization [35]. Therefore, in response to the low fermentation titers, long cultivation and fermentation cycles and extremely unstable metabolism of the original host, this research has pioneered a pathway for heterologous production of FDX.

Initially, through library construction and screening methods, we obtained a complete FDX BGC (pMSBBAC1-*fad*, over 100 kb) *in vitro*. Utilizing conjugative transfer of large plasmids and fermentation validation, we identified *S. albus* J1074 as the optimal host for FDX heterologous production. Based on this strain, we eliminated 6 redundant gene clusters and 2 genomic islands, while also integrating gene *vgb2* to augment the efficiency of O_2 utilization especially during the scale-up stage. The resulting chassis, D7-VHb, with a cumulative deletion of 358 kb fragments (5.25 % of the genome), possesses a more streamlined metabolic background, improved precursor and cofactor supply, and enhanced growth and heterologous expression capabilities for FDX. It is expected to become an excellent heterologous chassis for efficient production of natural products.

Subsequently, we embarked on an investigation into the compatibility of exogenous bio-bricks, FDX-BGC, and D7-VHb chassis. We screened 12 constitutive promoters with the objective of identifying the promoter most conducive to the overexpression of *fadR1*. Through XylE activity screening and promoter *in situ* replacement, we selected the optimal promoter, *rpsL(XC)*, to amplify the expression of positive regulator *fadR1* and the transcription of FDX-BGC, resulting in the strain D7-VHb-E*fad*. Utilizing this strain, we constructed an array of LuxR family “transcriptional factor libraries". Through FDX yield verification, it was discovered that the positive regulatory protein ScnRII of polyketide natamycin, derived from *Streptomyces chattanoogensis*, effectively enhanced the production of FDX in *S. albus*. Given that approximately 80 % of FDX accumulates intracellularly, leading to cytotoxicity and feedback inhibition, the expression of the transporter proteins FadT1 and FadT2, along with the addition of the macroporous resin XAD-16 to the culture medium, facilitated efficient transport and significantly increased the yield of FDX. Finally, by co-overexpressing *scnRII*, *fadT1T2*, and the pantothenate kinase gene *pank* in D7-VHb-E*fad*, combined with medium optimization and scale-up in a 5 L fermenter, we engineered a heterologous strain capable of stable, high, and rapid production of FDX.

5. Conclusion

In this study, fidaxomicin heterologous over-producing strains with high stability were constructed through a stepwise strategy including chassis construction, promoter engineering, regulatory activator screening, overexpression of efflux genes, and precursor synthesis genes. A genome-reduced *Streptomyces albus* D7-VHb was rationally constructed by combined strategy, and the chassis exhibited several emergent and excellent performances for heterologous expression of secondary metabolite. Based on this chassis, heterologous synthesis of FDX was achieved for the first time. Through combinatorial metabolic engineering strategy, we then developed a strain, D7-VHb-E*fad*-Com, that reached a yield of 384 mg/L in 5 L fermenter fermentation, which was approximately 15-fold higher than native strain YP-1. Moreover, D7-VHb-E*fad*-Com displayed superior genetic stability characteristics

and a shorter growth and fermentation cycle (2–3 days on solid media, 5 days in liquid) compared to the original wild-type strain YP-1 and high-yield strain YP-2 (6–8 days on solid media, 8 days in liquid). For the first time, we have constructed a biosynthesis system capable of stable, high and rapid heterologous production of fidaxomicin.

Ethics approval

This article does not contain any studies with human participants or experimental animals performed by any of the authors.

CRediT authorship contribution statement

Huang Xie: Conceptualization, Methodology, Formal analysis, Investigation, Visualization, Writing – original draft. **Yi-Ting Su:** Methodology, Writing – review & editing, Investigation. **Qing-Ting Bu:** Methodology, Writing – review & editing, Investigation. **Yue-Ping Li:** Writing – review & editing, Investigation. **Qing-Wei Zhao:** Investigation. **Yi-Ling Du:** Conceptualization, Methodology, Project administration, Resources, Supervision, Validation, Writing – original draft, Writing – review & editing. **Yong-Quan Li:** Conceptualization, Funding acquisition, Methodology, Project administration, Resources, Supervision, Validation, Writing – original draft, Writing – review & editing.

Declaration of competing interest

All authors have approved the manuscript for submission and we declare that we have no competing interests.

Acknowledgements

This work was supported by the National Key R&D Program of China (grant number 2019YFA09005400) and the Zhejiang Provincial Natural Science Foundation of China (grant number LQ21C010002).

Appendix A. Supplementary data

Supplementary data to this article can be found online at https://doi.org/10.1016/j.synbio.2024.06.004.

References

[1] Dorst A, Gademann K. Chemistry and biology of the clinically used macrolactone antibiotic fidaxomicin. Helv Chim Acta 2020;103(4):e2000038. https://doi.org/10.1002/hlca.202000038.

[2] Cornely OA, Nathwani D, Ivanescu C, Odufowora-Sita O, Retsa P, Odeyemi IA. Clinical efficacy of fidaxomicin compared with vancomycin and metronidazole in Clostridium difficile infections: a meta-analysis and indirect treatment comparison. J Antimicrob Chemother 2014;69(11):2892–900. https://doi.org/10.1093/jac/dku261.

[3] Tashiro S, Mihara T, Sasaki M, Shimamura C, Shimamura R, Suzuki S, et al. Oral fidaxomicin versus vancomycin for the treatment of *Clostridioides difficile* infection: a systematic review and meta-analysis of randomized controlled trials. J Infect Chemother 2022. https://doi.org/10.1016/j.jiac.2022.08.008.

[4] Biedenbach D J, Ross JE, Putnam SD, Jones RN. *In vitro* activity of fidaxomicin (OPT-80) tested against contemporary clinical isolates of *Staphylococcus* spp. and *Enterococcus* spp. Antimicrob Agents Chemother 2010;54(5):2273–5. https://doi.org/10.1128/aac.00090-10.

[5] Hattori H, Kaufmann E, Miyatake-Ondozabal H, Berg R, Gademann K. Total synthesis of tiacumicin A. Total synthesis, relay synthesis, and degradation studies of fidaxomicin (tiacumicin B, lipiarmycin A3). J Org Chem 2018;83(13):7180–205. https://doi.org/10.1021/acs.joc.8b00101.

[6] Xiao Y, Li S, Niu S, Ma L, Zhang G, Zhang H, et al. Characterization of tiacumicin B biosynthetic gene cluster affording diversified tiacumicin analogues and revealing a tailoring dihalogenase. J Am Chem Soc 2011;133(4):1092–105. https://doi.org/10.1021/ja109445q.

[7] Li Y-P, Yu P, Li J-F, Tang Y-L, Bu Q-T, Mao X-M, et al. FadR1, a pathway-specific activator of fidaxomicin biosynthesis in *Actinoplanes deccanensis* Yp-1. Appl Microbiol Biotechnol 2019;103:7583–96. https://doi.org/10.1007/s00253-019-09949-y.

[8] Li Y-P, Bu Q-T, Li J-F, Xie H, Su Y-T, Du Y-L, et al. Genome-based rational engineering of *Actinoplanes deccanensis* for improving fidaxomicin production and genetic stability. Bioresour Technol 2021;330:124982. https://doi.org/10.1016/j.biortech.2021.124982.

[9] Liu J, Wang X, Dai G, Zhang Y, Bian X. Microbial chassis engineering drives heterologous production of complex secondary metabolites. Biotechnol Adv 2022;59:107966. https://doi.org/10.1016/j.biotechadv.2022.107966.

[10] Xie H, Ruan J-Y, Bu Q-T, Li Y-P, Su Y-T, Zhao Q-W, et al. Transcriptional regulation of the fidaxomicin gene cluster and cellular development in *Actinoplanes deccanensis* YP-1 by the pleiotropic regulator MtrA. Microbiol Spectr 2023:e02702–23. https://doi.org/10.1128/spectrum.02702-23.

[11] Tan G-Y, Deng K, Liu X, Tao H, Chang Y, Chen J, et al. Heterologous biosynthesis of spinosad: an omics-guided large polyketide synthase gene cluster reconstitution in *Streptomyces*. ACS Synth Biol 2017;6(6):995–1005. https://doi.org/10.1021/acssynbio.6b00330.

[12] Huang S, Li N, Zhou J, He J. Construction of a new bacterial artificial chromosome (BAC) vector for cloning of large DNA fragments and heterologous expression in Streptomyces. Weishengwu Xuebao 2012;52(1):30–7.

[13] Flett F, Mersinias V, Smith CP. High efficiency intergeneric conjugal transfer of plasmid DNA from *Escherichia coli* to methyl DNA-restricting *streptomycetes*. FEMS (Fed Eur Microbiol Soc) Microbiol Lett 1997;155(2):223–9. https://doi.org/10.1111/j.1574-6968.1997.tb13882.x.

[14] Wang H, Li Z, Jia R, Hou Y, Yin J, Bian X, et al. RecET direct cloning and Redαβ recombineering of biosynthetic gene clusters, large operons or single genes for heterologous expression. Nat Protoc 2016;11(7):1175–90. https://doi.org/10.1038/nprot.2016.054.

[15] Li L, Liu X, Jiang W, Lu Y. Recent advances in synthetic biology approaches to optimize production of bioactive natural products in actinobacteria. Front Microbiol 2019;10:2467. https://doi.org/10.3389/fmicb.2019.02467.

[16] Bu QT, Yu P, Wang J, Li ZY, Chen XA, Mao XM, et al. Rational construction of genome-reduced and high-efficient industrial *Streptomyces* chassis based on multiple comparative genomic approaches. Microb Cell Factories 2019;18(1):16. https://doi.org/10.1186/s12934-019-1055-7.

[17] Zaburannyi N, Rabyk M, Ostash B, Fedorenko V, Luzhetskyy A. Insights into naturally minimised *Streptomyces albus* J1074 genome. BMC Genom 2014;15:1–11. https://doi.org/10.1186/1471-2164-15-97.

[18] Gomez-Escribano JP, Bibb MJ. Engineering *Streptomyces coelicolor* for heterologous expression of secondary metabolite gene clusters. Microb Biotechnol 2011;4(2):207–15. https://doi.org/10.1111/j.1751-7915.2010.00219.x.

[19] Komatsu M, Komatsu K, Koiwai H, Yamada Y, Kozone I, Izumikawa M, et al. Engineered *Streptomyces avermitilis* host for heterologous expression of biosynthetic gene cluster for secondary metabolites. ACS Synth Biol 2013;2(7):384–96. https://doi.org/10.1021/sb3001003.

[20] Blin K, Shaw S, Kloosterman AM, Charlop-Powers Z, Van Wezel GP, Medema MH, et al. antiSMASH 6.0: improving cluster detection and comparison capabilities. Nucleic Acids Res 2021;49(W1):W29–35. https://doi.org/10.1093/nar/gkab335.

[21] Horng YT, Chang KC, Chien CC, Wei YH, Sun YM, Soo PC. Enhanced polyhydroxybutyrate (PHB) production via the coexpressed *phaCAB* and *vgb* genes controlled by arabinose P_{BAD} promoter in *Escherichia coli*. Lett Appl Microbiol 2010;50(2):158–67. https://doi.org/10.1111/j.1472-765X.2009.02772.x.

[22] Mirończuk AM, Kosiorowska KE, Biegalska A, Rakicka-Pustułka M, Szczepańczyk M, Dobrowolski A. Heterologous overexpression of bacterial hemoglobin VHb improves erythritol biosynthesis by yeast *Yarrowia lipolytica*. Microb Cell Factories 2019;18:1–8. https://doi.org/10.1186/s12934-019-1231-9.

[23] Lyu Z-Y, Bu Q-T, Fang J-L, Zhu C-Y, Xu W-F, Ma L, et al. Improving the yield and quality of daptomycin in *Streptomyces roseosporus* by multilevel metabolic engineering. Front Microbiol 2022;13:872397. https://doi.org/10.3389/fmicb.2022.872397.

[24] Liu J, Zhou H, Yang Z, Wang X, Chen H, Zhong L, et al. Rational construction of genome-reduced Burkholderiales chassis facilitates efficient heterologous production of natural products from proteobacteria. Nat Commun 2021;12(1):4347. https://doi.org/10.1038/s41467-021-24645-0.

[25] Bu Q-T, Li Y-P, Xie H, Wang J, Li Z-Y, Chen X-A, et al. Comprehensive dissection of dispensable genomic regions in *Streptomyces* based on comparative analysis approach. Microb Cell Factories 2020;19:1–12. https://doi.org/10.1186/s12934-020-01359-4.

[26] Li S, Li Z, Pang S, Xiang W, Wang W. Coordinating precursor supply for pharmaceutical polyketide production in *Streptomyces*. Curr Opin Biotechnol 2021;69:26–34. https://doi.org/10.1016/j.copbio.2020.11.006.

[27] Bilyk B, Horbal L, Luzhetskyy A. Chromosomal position effect influences the heterologous expression of genes and biosynthetic gene clusters in *Streptomyces albus* J1074. Microb Cell Factories 2017;16:1–8. https://doi.org/10.1186/s12934-016-0619-z.

[28] Zhang XS, Luo HD, Tao Y, Wang YY, Jiang XH, Jiang H, et al. FkbN and Tcs7 are pathway-specific regulators of the FK506 biosynthetic gene cluster in Streptomyces tsukubaensis L19. J Ind Microbiol Biotechnol 2016;43(12):1693–703. https://doi.org/10.1007/s10295-016-1849-0.

[29] He W, Wang W, Ma J, Zheng G, Zimin AA, Jiang W, et al. Crossregulation of rapamycin and elaiophylin biosynthesis by RapH in *Streptomyces rapamycinicus*. Appl Microbiol Biotechnol 2022;106(5):2147–59. https://doi.org/10.1007/s00253-022-11847-9.

[30] Santos-Aberturas J, Payero TD, Vicente CM, Guerra SM, Canibano C, Martin JF, et al. Functional conservation of PAS–LuxR transcriptional regulators in polyene macrolide biosynthesis. Metab Eng 2011;13(6):756–67. https://doi.org/10.1016/j.ymben.2011.09.011.

[31] Zhang N, Dong Y, Zhou H, Cui H. Effect of PAS-LuxR family regulators on the secondary metabolism of *streptomyces*. Antibiotics 2022;11(12):1783. https://doi.org/10.3390/antibiotics11121783.

[32] Mandakh A, Niraula NP, Kim E-P, Sohng J-K. Identification and characterization of a pantothenate kinase (PanK-sp) from *Streptomyces peucetius* ATCC 27952. J Microbiol Biotechnol 2010;20(12):1689–95. https://doi.org/10.4014/jmb.1007.07058.

[33] Ko Y-S, Kim JW, Lee JA, Han T, Kim GB, Park JE, et al. Tools and strategies of systems metabolic engineering for the development of microbial cell factories for chemical production. Chem Soc Rev 2020;49(14):4615–36. https://doi.org/10.1039/D0CS00155D.

[34] Gu B, Kim DG, Kim D-K, Kim M, Kim HU, Oh M-K. Heterologous overproduction of oviedomycin by refactoring biosynthetic gene cluster and metabolic engineering of host strain *Streptomyces coelicolor*. Microb Cell Factories 2023;22(1):212. https://doi.org/10.1186/s12934-023-02218-8.

[35] Li Z, Huang P, Wang M, Wang X, Wang L, Kong D, et al. Stepwise increase of thaxtomins production in *Streptomyces albidoflavus* J1074 through combinatorial metabolic engineering. Metab Eng 2021;68:187–98. https://doi.org/10.1016/j.ymben.2021.10.008.